DOI: 10.1002/ejic.200601236

A New Pentadentate Ligand Forms Both a Di- and a Mononuclear Mn^{II} Complex: Electrochemical, Spectroscopic and Superoxide Dismutase Activity Studies

Federico Cisnetti,[a,b] Anne-Sophie Lefèvre,[a,b] Régis Guillot,[b,c] François Lambert,[a,b] Guillaume Blain,[b,c] Elodie Anxolabéhère-Mallart,[b,d] and Clotilde Policar*[a,b]

Keywords: Manganese(II) / Enzyme models / SOD mimic / N,O ligands / Bioinorganic chemistry

The X-ray crystal structure of the dinuclear complex [**1**$(PF_6)_2$] derived from a new ligand bearing both imidazole and phenolato moieties, namely *N*-(2-hydroxybenzyl)-*N*,*N*′-bis[2-(*N*-methylimidazolyl)methyl]ethane-1,2-diamine (LH), is described and its properties in organic solvent (CH_3CN) investigated (EPR, electrochemistry). [**1**$(PF_6)_2$] is shown to be a mononuclear Mn^{II} species in aqueous solution and displays an efficient SOD-like activity, as measured by the McCord–Fridovich assay performed both in conventional phosphate buffer and in a noncoordinating buffer (PIPES).

Introduction

Superoxide is known to be a toxic reactive oxygen species (ROS) involved in oxidative stress[1–4] and is considered to be responsible for several pathologic situations. Under normal conditions, its concentration is kept low (8–40 pM)[5,6] by metalloenzymes, known as superoxide dismutases (SODs), that catalyze its dismutation. As the therapeutic use of purified enzymes has major drawbacks,[3] different low molecular weight complexes have been synthesized for this purpose using either copper, iron, manganese, or cobalt ions. As Mn derivatives do not lead to Fenton chemistry, special interest has been devoted to Mn complexes (oxidation states II, III, or IV) as antisuperoxide agents for possible therapeutic use.[2–4] Free Mn^{II}[7–9] or Mn coordinated to salen derivatives,[8,10–12] cyclic polyamines,[3,13–19] tri- or dipodal ligands,[20–28] 1,2-ethanediamine-based ligands,[29–32] desferrioxamine derivatives[13,33,34] polyaminocarboxylato[35–37] or polycarboxylato ligands,[38] peptides,[39–41] as well as Mn^{III} porphyrins,[42–47] or dinuclear biliverdin manganese complexes[48] have been reported to react with superoxide either as a true SOD mimetic or as a scavenger.

One of the goals of our research is the synthesis of bioactive complexes of therapeutic interest in the case of oxidative stress.[2–4] In the past few years we have synthesized a series of Mn complexes containing tripodal amines as tetradentate ligands that show an SOD-like activity, according to the results of the indirect McCord–Fridovich assay[24,27,28] and pulsed radiolysis experiments.[26,27] These complexes were designed as bio-inspired functional SOD mimics bearing in mind that the active site of Mn-based SODs has a trigonal-bipyramidal N_3O_2 core with three histidines, a monodentate aspartate, and an aqua or hydroxido ligand.[49]

Pentadentate ligands based on a 1,2-ethanediamine moiety are interesting alternatives to the previous tetradentate N-tripod series because they offer a larger number of possible variations.[50–52] We report here the synthesis of a complex with a new pentadentate ligand L [LH = *N*-(2-hydroxybenzyl)-*N*,*N*′-bis[2-(*N*-methylimidazolyl)methyl]ethane-1,2-diamine], which contains a 1,2-ethanediamine backbone bearing one phenol (mimicking the monodentate carboxylate present at the Mn-SOD active site) and two 1-methylimidazole groups (mimicking the histidine side-chains) as coordinating groups (Scheme 1). We describe the structure and solution characterization (EPR and UV/Vis spectroscopy, electrochemistry) of the dinuclear complex [(L)MnMn(L)]$(PF_6)_2$ [**1**$(PF_6)_2$] in organic solution and show that in aqueous solution this complex is in the monometallic form $[(L)Mn]^+$ (EPR, cyclic voltammetry). The SOD-like activity of the $[(L)Mn]^+$ species has been measured in aqueous solution using the conventional McCord–

[a] Equipe de Chimie Biorganique et Bioinorganique, Institut de Chimie Moléculaire et des Matériaux d'Orsay, Univ. Paris-Sud, UMR 8182,
91405 Orsay, France
E-mail: cpolicar@icmo.u-psud.fr
[b] Institut de Chimie Moléculaire et des Matériaux d'Orsay, CNRS, UMR 8182,
91405 Orsay, France
[c] Institut de Chimie Moléculaire et des Matériaux d'Orsay, Univ. Paris-Sud, UMR 8182,
91405 Orsay, France
[d] Equipe de Chimie Inorganique, Institut de Chimie Moléculaire et des Matériaux d'Orsay, Univ. Paris-Sud, UMR 8182,
91405 Orsay, France
Supporting information for this article is available on the WWW under http://www.eurjic.org or from the author.

Fridovich test under noncoordinating conditions. The good activity found is consistent with the redox potential of the $[(L)Mn]^+$ species measured by CV.

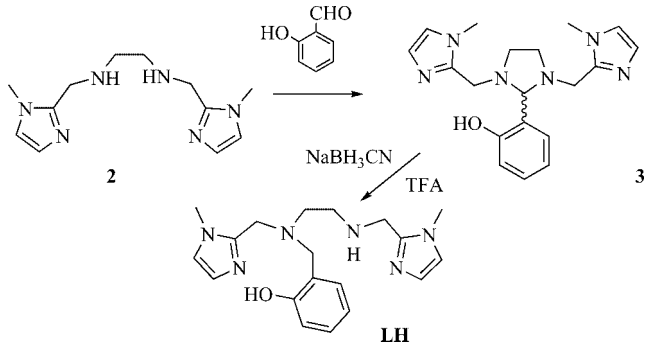

Scheme 1. Synthetic route to LH.

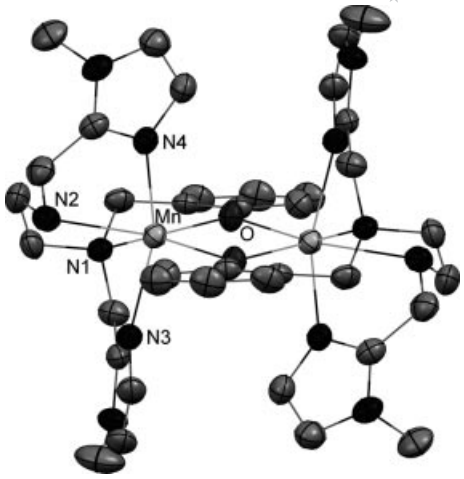

Figure 1. Ellipsoid plot of the centrosymmetric cationic moiety **1**, produced with Mercury 1.4.2.[56] Ellipsoids are drawn at 50% probability level. PF_6^- and H atoms have been omitted for clarity.

Results and Discussion

The synthesis of LH is straightforward. *N*,*N*′-Bis[2-(*N*-methylimidazolyl)methyl]ethane-1,2-diamine (**2**) was obtained by a conventional two-step reductive amination procedure starting from 1-methyl-2-imidazolecarboxaldehyde[53] and 1,2-ethanediamine, as published elsewhere.[54] The dissymmetric pentadentate ligand containing a phenolic group was then obtained by treating **2** with salicylaldehyde to obtain the aminal **3** (Scheme 1), which was reductively opened with $NaBH_3CN$ in the presence of an acid.[55] The whole synthesis proceeded with high yields. The reaction of crude LH with $MnBr_2$ in warm methanolic solution led to the formation of a Mn^{II} complex. Crystals suitable for X-ray diffraction were grown by cooling this solution to room temperature under argon in the presence of hexafluorophosphate anion.

Table 1. Selected bond distances [Å] and angles [°] in the cationic complex **1**. The uncertainties correspond to 2σ (σ is given in the cif file).

N4–Mn	2.205(8)	O–Mn–O	79.2(2)	O–Mn–N2	128.5(2)
N2–Mn	2.420(8)	O–Mn–N4	94.2(3)	N1–Mn–N2	76.8(3)
N1–Mn	2.354(8)	N4–Mn–N2	71.0(3)	N4–Mn–N1	113.7(3)
O–Mn	2.111(6)	N1–Mn–O	83.1(1)	N3–Mn–O	109.9(3)
O′–Mn	2.172(6)	N1–Mn–N3	72.8(2)	N3–Mn–N2	86.0(3)
N3–Mn	2.226(8)	N3–Mn–O	89.0(2)	N4–Mn–O	97.1(3)

Description of the Structure

The X-ray crystal structure of this complex revealed it to be dinuclear with the formula $[(L)MnMn(L)](PF_6)_2$ [**1**$(PF_6)_2$]. A view of cation **1** is presented in Figure 1. This cation is dinuclear and centrosymmetric with a central di-μ-phenolato Mn_2O_2 diamond core. Selected bond lengths and angles are reported in Table 1.

Each Mn^{II} ion is hexacoordinate, with four nitrogen atoms of the anionic form L^- of the ligand and two oxygen atoms from the phenolato groups, the first one from the same ligand and the other one from the ligand chelating the second Mn^{II} ion. The Mn environment departs from that of a regular octahedron (see Table 1). The longest coordination bond is that to the secondary amine N2, and the N2–Mn–O angle is much larger than the ideal value for an octahedron. These distances and deformations are similar to those reported for similar Mn^{II} dinuclear compounds,[50,51] in particular to the dinuclear phenolate-bridged dication $[(mL')Mn^{II}Mn^{II}(mL')]^{2+}$ [mL′H = *N*-(2-hydroxybenzyl)-*N*′-methyl-*N*,*N*′-bis(2-pyridylmethyl)-ethane-1,2-diamine].[51] Such a dinuclear structure in which manganese atoms show a distorted octahedral geometry is in line with the fact that Mn^{II} complexes, due to their half-filled d^5 shell, have no electronic coordination preference.[57]

EPR Spectroscopy

The X-band EPR spectrum of a 1.1 mM acetonitrile solution of **1**$(PF_6)_2$ in the presence of 0.1 M tetrabutylammonium perchlorate was recorded at 7 K in both the perpendicular and parallel modes. The spectrum recorded in the perpendicular mode exhibits features extending from 0 to 800 mT (Figure 2), which arise from the superimposition of the signal of the five paramagnetic spin states S= 1 to 5 and is characteristic of dinuclear Mn^{II} complexes.[51,52,58–63] The band at around 260 mT (B) shows a nice hyperfine structure with a field separation between two lines of about 41 G (see insert Figure 2), which is typical of dinuclear $Mn^{II}Mn^{II}$ complexes. Increasing the temperature induced only slight modifications in the spectral profile [the band at around 204 mT (A) and the intensity of the signal at 330 mT (C)]. Unlike previous observations with a dinuclear bis-μ-phenolato $Mn^{II}Mn^{II}$ complex with a J-value of $-1.5\ cm^{-1}$,[50] the intensities do not reach a maximum but decrease on increasing the temperature from 7 to 30 K (see Figure 2). This thermal behavior is consistent with the very

weak *J*-value estimated from the measurement of the magnetic susceptibility as a function of temperature (see Experimental Section).

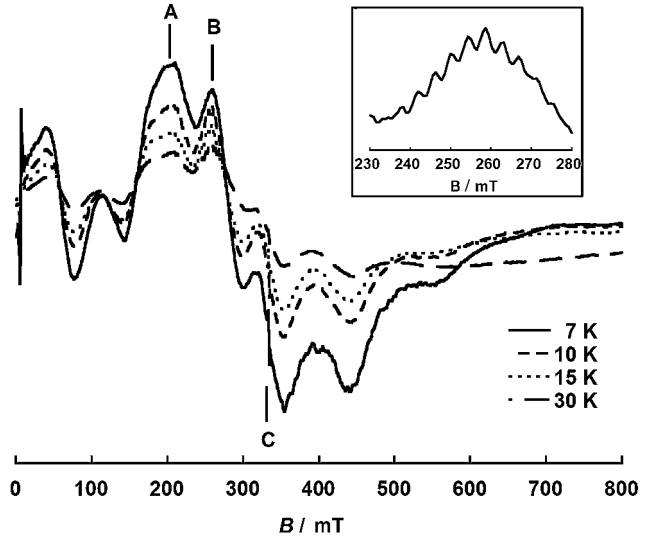

Figure 2. X-band EPR spectrum of $\mathbf{1}(PF_6)_2$ (1.1 mM in CH_3CN containing 0.1 M tetrabutylammonium perchlorate) at 7 K. Microwave frequency: 9.63 GHz; microwave power: 2 mW; modulation amplitude: 0.5 mT; modulation frequency: 100 kHz; gain: 40 dB.

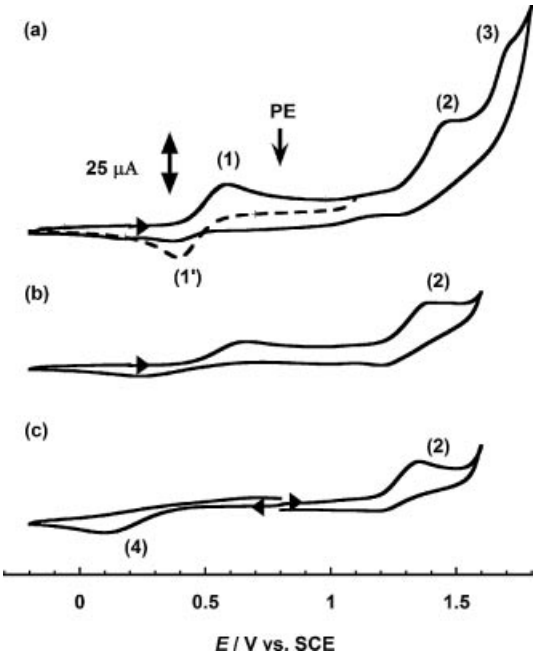

Figure 3. Cyclic voltammograms of $\mathbf{1}(PF_6)_2$ (1.1 mM in CH_3CN with 0.1 M tetrabutylammonium perchlorate) under argon (v = 0.1 $V s^{-1}$; working electrode: glassy carbon; counter electrode: Pt wire; reference electrode: $Ag/AgClO_4$) at 20 (a) –25 (b), and –25 °C after electrolysis at E = +0.8 V vs. SCE (c). PE = potential of the preparative electrolysis.

Electrochemical Access to Mn^{III}

The cyclic voltammogram of a 1.1 mM acetonitrile solution of $\mathbf{1}(PF_6)_2$ is shown in Figure 3. The CV trace shows a well-defined anodic wave (wave 1 in Figure 3a) at E_p^a = 0.58 V vs. SCE and a well-defined cathodic wave on the reverse scan at E_p^c = 0.39 V vs. SCE (wave 1′). The difference between these two values ($\Delta E_p = E_p^a - E_p^c$) of 190 mV is indicative of a slow electron transfer. A similar behavior has previously been reported for related dinuclear $Mn^{II}Mn^{II}$ complexes with pyridine instead of imidazole moieties.[50] Controlled potential coulometry performed at +0.8 V vs. SCE indicated a one electron per Mn process for the first oxidation. Thus, the first anodic wave (1/1′; $E_{1/2}$ = 0.485 V vs. SCE)[64] can be attributed to a two-electron $Mn^{II}Mn^{II} \rightarrow Mn^{III}Mn^{III}$ process. This oxidation occurs at lower potential than that reported for the pyridine-containing ligand mL′[51] as the imidazole group has a higher electron-donating effect than pyridine, which leads to greater stabilization of the Mn^{III} oxidation state.

Two other anodic peaks (labeled 2 and 3 in Figure 3, a) are observed at E_p^a = 1.4 and 1.7 V vs. SCE respectively. These second and third oxidation processes are tentatively attributed to Mn^{III} to Mn^{IV} and phenolato oxidation processes.[50,65]

In an effort to determine the exact nature of the resulting Mn^{III} species, a controlled potential electrolysis was performed at +0.8 V vs. SCE at –25 °C. Aliquots of the electrolyzed solution were collected during the course of the electrolysis and their UV/Vis absorption (Figure 4) and EPR spectra recorded. Figure 3 shows the cyclic voltammograms recorded at –25 °C before (Figure 3, b) and after (Figure 3, c) complete electrolysis at +0.8 V vs. SCE. After electrolysis one anodic process was detected at E_p^a = +1.35 V vs. SCE

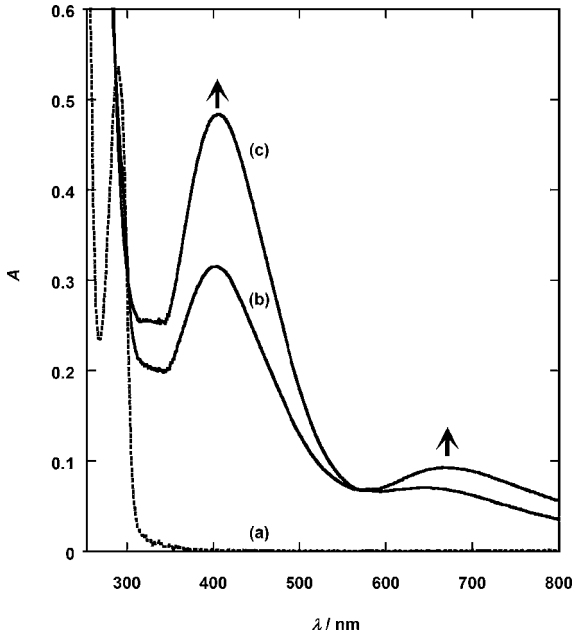

Figure 4. Evolution of the UV/Vis spectrum of $\mathbf{1}(PF_6)_2$ (1.1 mM acetonitrile solution) during bulk electrolysis at E = 0.8 V vs. SCE before electrolysis (a), after 0.5 electron/Mn (b), and after 1 electron/Mn (c) at room temperature. Path length = 0.1 cm.

and one irreversible cathodic process at E_p^c = +0.1 V vs. SCE when scanning towards low potential (labeled 4 in Figure 3, c).

As expected for a Mn^{II} oxidation state, the UV/Vis spectrum of **1** (Figure 4) only shows features in the UV region (λ_1 = 287 nm, ε_1 = 4909 $M^{-1}cm^{-1}$) associated with π–π* transitions of the ligand. The colorless solution turns pink upon oxidation at 0.8 V and two new absorption bands appear at λ_2 = 403 and λ_3 = 672 nm. Based on a complete conversion of the initial Mn^{II} into Mn^{III}, the extinction coefficients calculated per Mn ion are ε_2 = 2181 and ε_3 = 432 $M^{-1}cm^{-1}$. Similar bands have been reported in the literature for mononuclear Mn^{III} complexes[66] or dinuclear $Mn^{III}Mn^{III}$ complexes with phenolato/pyridine ligands.[65] The band at 403 nm can therefore be attributed to a phenolato to Mn^{III} LMCT transition. Due to the lower value of its extinction coefficient, and previous reports in the literature, the band at 672 nm can be attributed to a d-d transition.[67,68]

The intensity of the X-band perpendicular mode EPR spectrum of the initial $Mn^{II}Mn^{II}$ complex decreased during the course of the electrolysis. After completion of the electrolysis (1 electron/1 Mn), the pink solution was EPR-silent in the perpendicular mode (data not shown), as expected for a Mn^{III} complex. Unfortunately, no signal was detected when a parallel mode EPR spectrum was recorded for the pink solution.

The above-mentioned experimental data confirm the Mn^{III} oxidation state of the oxidized species, although the exact nature of the Mn^{III} species remains uncertain as a dinuclear bis-μ-phenolato $Mn^{III}Mn^{III}$ complex is likely to be unstable in solution. As reported previously in the literature, the bis-μ-phenolato bridge can easily break and generate two mononuclear $[(L)Mn^{III}(S)]^{2+}$ complexes, where S can either be a water molecule or a solvent molecule.[51] It should be noted that wave 2 disappeared upon addition of 2,6-lutidine[69] and a new anodic wave appeared at 1.02 V vs. SCE. Based on these results (see Figure S1 in the electronic supporting information), wave 2 can be assigned to the $[(L)Mn^{III}(OH_2)]^{2+}/[(L)Mn^{IV}(OH_2)]^{3+}$ oxidation process and the wave at 1.02 V to the $[(L)Mn^{III}(OH)]^{+}/[(L)Mn^{IV}(OH)]^{2+}$ oxidation process as deprotonation of the aqua complex lowers the Mn^{IV}/Mn^{III} redox potential. Wave 4 can tentatively be assigned to reduction of the mononuclear $[(L)Mn^{III}(OH_2)]^{2+}$ species into $[(L)Mn^{II}(OH_2)]^{+}$.

Nature of the Complex in Water

Cyclic voltammetry and the EPR spectrum recorded in CH_3CN are consistent with a dinuclear $[(L)MnMn(L)]^{2+}$ species (**1**; see above). In order to investigate the behavior of the complex in aqueous solution, electrochemistry and EPR spectra were recorded in a noncoordinating buffer, namely piperazine-*N*,*N*′-bis(2-ethanesulfonic acid) (PIPES; 50 mM, pH 7.5).[38,70]

The EPR spectra of a 1 mM solution in PIPES (Figure 5) displays a large six-line signal at g = 2 (ΔB_{av} = 96 G) characteristic of a mononuclear Mn^{II} center. The low-intensity signal at $g \approx 3.94$ is typical for distorted Mn^{II} environ-

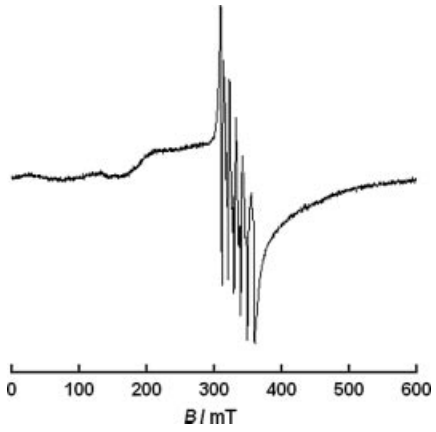

Figure 5. X-band EPR spectra of $\mathbf{1}(PF_6)_2$ (10^{-3} M in 50 mM aqueous PIPES buffer, pH 7.5). Microwave frequency: 9.38 GHz; microwave power: 2.0 mW; modulation amplitude: 0.5 mT; modulation frequency: 100 kHz; gain: 20 dB.

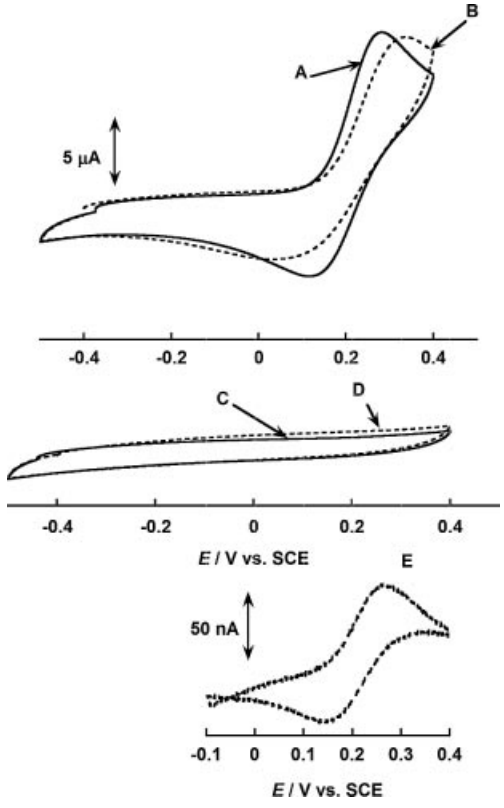

Figure 6. Cyclic voltammograms in aqueous solution: (A) $\mathbf{1}(PF_6)_2$ (10^{-3} M) in aqueous PIPES buffer (pH 7.5, 50 mM) and (B) in aqueous phosphate buffer (pH 7.8, 50 mM); (**C**) $MnCl_2$ (10^{-3} M) in aqueous PIPES buffer (pH 7.5, 50 mM) and (D) in aqueous phosphate buffer (pH 7.8, 50 mM); (E) $\mathbf{1}(PF_6)_2$ (10^{-5} M) in aqueous PIPES buffer (pH 7.5, 50 mM; the signal recorded for pure PIPES buffer has been subtracted). Working electrode: glassy carbon; counter electrode: Pt wire; reference electrode: SCE.

ments.[71–74] This species will be labeled $[(L)Mn]^+$ in the following discussion, although there is probably a water molecule coordinated to the metal center.

Figure 6 shows the cyclic voltammogram of $[\mathbf{1}(PF_6)_2]$ dissolved in PIPES (1 mM; trace A). Trace A displays a well-defined anodic wave at $E_p^a = 0.282$ V vs. SCE and a well-defined cathodic wave on the reverse scan at $E_p^c = 0.116$ V vs. SCE ($E_{1/2} = 0.199$ V vs. *SCE* and $\Delta E_p = 165$ mV). Neither $MnCl_2$ (trace C in Figure 6) nor $Mn(ClO_4)_2$ (not shown) dissolved in PIPES show any wave at these potentials. A similar voltammogram, although less reversible, was recorded for $\mathbf{1}(PF_6)_2$ dissolved in pH 7.8 phosphate buffer (see Figure 6 trace B, $E_{1/2} = 0.184$ V vs. SCE; $E_p^a = 0.334$ V, $E_p^c = 0.037$ V vs. SCE; $\Delta E_p = 331$ mV).

Taken together, the EPR spectra and cyclic voltammograms unambiguously indicate that in aqueous solution the metal-containing species is therefore mononuclear Mn^{II} (EPR) coordinated to L (the CV signature is different from that of uncoordinated Mn^{2+}).

The nature of this species was also investigated at 10^{-5} M both by CV and EPR spectroscopy. The electrochemical signature of the mononuclear $[(L)Mn]^+$ complex was still observed, with an intensity two orders of magnitude smaller, as expected for a concentration that is two orders of magnitude smaller. This indicates that no de-coordination occurs at this low concentration and is also consistent with the electrospray mass spectrometry analysis of a 10^{-5} M aqueous solution of $\mathbf{1}(PF_6)_2$, which shows a peak assigned to the mononuclear $[(L)Mn]^+$ cation (with spacings in the *M* multiplet equal to 1) and no peaks assignable to either **1** (at $M_{dinuclear}/2$, with expected spacings of 1/2) or to monocationic adducts.

SOD-Like Activity in Aqueous Buffer

The mononuclear $[(L)Mn]^+$ cation was tested for its superoxide dismutase like activity using the McCord–Fridovich assay,[34,75] as published previously,[24,27] with ferricytochrome c as the detector. Two different buffers, namely phosphate buffer (pH 7.8, 50 mM) and the noncoordinating buffer PIPES (pH 7.5, 50 mM), were used, as in a previous study by Fridovich et al.[38] To the best of our knowledge, the PIPES buffer has only been used in the original publication by Fridovich et al.[38] even though these conditions appear to be a good alternative to phosphate buffer conditions.

The complex $[(L)Mn]^+$ displays very similar SOD-like activity under both sets of conditions, as shown by the inhibition of the reduction of ferricytochrome c. As shown in Figure 7, the activity of the complex is different from that of Mn^{2+}_{aq} (see insert in Figure 7 and Table 2), which is consistent with the fact that the complex remains coordinated in dilute aqueous solution, as evidenced by the CV and ES-MS experiments at 10^{-5} M (see above).

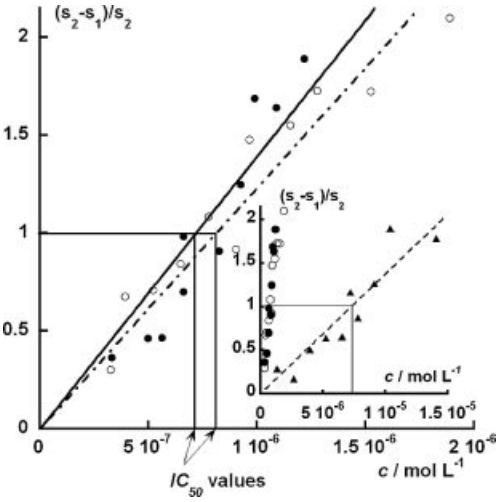

Figure 7. Determination of the IC_{50} value for $[(L)Mn]^+$ in PIPES buffer (50 mM, pH 7.5; exp. points: filled circles; linear curve fit: solid line) and phosphate buffer (50 mM, pH 7.8; exp. points: open circles; linear curve fit: dot-dashed line). Inset: comparison with $MnCl_2$ in 50 mM PIPES (exp. points: triangles; linear fit: dashed line). The assay was performed by recording the reduction of ferricytochrome c at 550 nm as a function of time. The slope of the line $A_{550nm} = f(t)$ before addition of the SOD mimic is s_1 and s_2 is the slope after addition of the SOD mimic. $(s_1 - s_2)/s_2$ was plotted against the complex concentration to provide a line, and the IC_{50} was then obtained for $(s_1 - s_2)/s_2 = 1$.[79]

Table 2. IC_{50} values.

	$IC_{50\ buffer}$[a,b]	k_{McCF} [$M^{-1}\,s^{-1}$][c]
Mn^{2+}_{aq} ($MnCl_2$)	$IC_{50\ PIPES} = (7.3 \pm 0.5) \times 10^{-6}$ M	–[d]
$[(L)Mn]^+$	$IC_{50\ PIPES} = (7.2 \pm 0.4) \times 10^{-7}$ M	–
	$IC_{50\ Phosphate} = (8.1 \pm 0.3) \times 10^{-7}$ M	$(7.0 \pm 0.3) \times 10^6$

[a] 50% Inhibition concentration. [b] Uncertainties were obtained from the fitting linearization procedure. [c] k_{McCF} values were recalculated from the IC_{50} value. [d] k_{McCF} was not recalculated as free Mn^{II} is known to be catalytically inactive.[2] See ref.[4] for a comparison with similar N_4O complexes.

IC_{50} values are dependent on the concentration of the detector, therefore in order to determine the activity we recalculated the apparent kinetic constant k_{McCF}.[27] At the IC_{50} value, the kinetics of the reduction of ferricytochrome c by superoxide is reduced by 50% as 50% of the superoxide is consumed by the ferricytochrome c and 50% by the complex (auto-dismutation being negligible in comparison). The apparent kinetic constant can thus be defined as $k_{McCF} = k_{detector} \times [detector]/IC_{50}$[27,76] and can be derived in the case of the phosphate buffer, for which the kinetic constant k_{cytC} has been measured [k_{cytC} (pH 7.8, 50 mM phosphate, 21 °C) = 2.6×10^5 $M^{-1}\,s^{-1}$].[77,78] The complex $[(L)Mn]^+$ therefore displays an apparent catalytic rate k_{McCF} of $(7.0 \pm 0.3) \times 10^6$ $M^{-1}\,s^{-1}$.

The activity reported here is one of the best reported for the series of Mn^{II} complexes with a similar coordination sphere (N/O coordination sphere with N from imidazole or pyridine and O from carboxylato or phenolato) reported by us and others,[23–25,27,28,80] which makes sense in light of the redox potential for the mononuclear $[(L)Mn]^+$ species mea-

sured in aqueous buffer. As the catalysis of the dismutation of superoxide is a redox process involving both Mn^{II} and Mn^{III} oxidation states, the potential of the Mn^{II}/Mn^{III} couple is a key parameter.[27] It should lie between the potential of the two couples O_2/O_2^- and O_2^-/H_2O_2 with the optimum being the midpoint, that is 0.12 V vs. SCE (at pH 7), which is the case for all SODs.[27,81,82] The mononuclear complex $[(L)Mn]^+$ ($E_{1/2}$ = 0.199 V vs. SCE) fulfills this requirement.

Conclusions

The dinuclear bis-μ-phenolato complex $[(L)Mn^{II}Mn^{II}(L)](PF_6)_2$ [**1**$(PF_6)_2$], which contains a new amino/imidazole pentadentate N_4O ligand, has been synthesized and its structure resolved by X-ray diffraction. An X-band EPR spectroscopy investigation has confirmed the dinuclear nature of the compound in acetonitrile solution. The cyclic voltammogram of **1** in acetonitrile solution displays a quasi-reversible anodic process at $E_{1/2}$ = 0.485 V vs. SCE assigned to the two-electron oxidation of the $Mn^{II}Mn^{II}$ species into the $Mn^{III}Mn^{III}$ species. The electrochemical formation of a Mn^{III} species has been followed by UV/Vis and EPR spectroscopy. In aqueous solution, the dinuclear complex has been shown to be converted into a cationic mononuclear complex $[(L)Mn]^+$ with a redox potential of +0.199 V vs. SCE. Its superoxide dismutase-like (SOD-like) activity has been evaluated by the means of the McCord–Fridovich assay. The complex has a potent SOD-like activity, with an apparent catalytic rate, k_{McCF}, of $(7.0 \pm 0.3) \times 10^6$ $M^{-1}s^{-1}$. The development of manganese complexes based on 1,2-ethanediamine is of interest for the synthesis of efficient SOD mimics.

Experimental Section

All reagents were bought from Acros Organics and used without further purification. 1-Methyl-imidazole carboxaldehyde was synthesized according to Iberson et al.[53] *N*,*N*′-Bis[2-(*N*-methylimidazolyl)methyl]ethane-1,2-diamine was synthesized according to Laronde et al.[54] NMR spectra were recorded with a Bruker AV360 or DRX300 spectrometer. IR spectra (KBr pellets) were recorded with a Bruker IFS 66 FT-IR spectrometer. Microanalysis was performed by the Service de Microanalyse de l'ICSN (Gif-sur-Yvette, France) for C,H,N, and by the Service Central d'Analyse du CNRS (Vernaison, France) for other elements.

Electrospray-ionization mass spectra were recorded with a Finnigan Mat 95S in the BE configuration at low resolution. X-band EPR spectra were recorded with a Bruker ELEXSYS 500 spectrometer fitted with an Oxford Instrument continuous-flow liquid helium or nitrogen cryostat and a temperature control system. UV/Vis spectra were recorded with a Cary 300 Bio Spectrophotometer with a 0.1-cm optical path quartz cuvette. The McCord–Fridovich assay was performed on the same apparatus at 25 °C and with a 1-cm optical path quartz cuvette. All electrochemical experiments were performed under argon. Cyclic voltammetry and coulometry were performed with a M273 EGG PAR potentiostat. The counter electrode for cyclic voltammetry was a Pt wire and the working electrode a glassy carbon disk, which was carefully polished before each voltammogram with a 1-μm diamond paste, sonicated in an ethanol bath, and then washed carefully with ethanol and dried. The counter electrode for bulk electrolysis was a piece of Pt separated from the rest of the solution with a fritted bridge. The working electrode was a Pt gauze (about 20 cm^2). The solvent used was (a) distilled acetonitrile with tetrabutylammonium perchlorate added to obtain a 0.1 M supporting electrolyte or (b) doubly distilled water with either phosphate or PIPES buffer (50 mM). The reference electrode was (a) an $Ag/AgClO_4$ electrode (0.3 V vs. SCE) for experiments in CH_3CN and (b) an SCE electrode for experiments in water. In both cases, the reference electrode was isolated from the rest of the solution with a fritted bridge. Temperature regulation (20 °C) was ensured by a Julabo circulation cryostat.

2-(2-Hydroxybenzyl)-*N*,*N*′-bis[2-(*N*-methylimidazolyl)methyl]imidazolidine (3): A solution of compound **2**[54] (0.500 g, 2.01 mmol, 1 equiv.) in absolute ethanol (10 mL) was mixed with salicylaldehyde (0.246 g, 215 μL, 2.01 mmol, 1 equiv.). After stirring the reaction mixture for 24 h at ambient temperature, anhydrous sodium sulfate (0.5 g) was added to eliminate water. After stirring for a further 30 min the reaction mixture was filtered and the solvent evaporated to give the crude product as a yellow oil (0.700 g, quantitative yield). ^{1}H NMR (360 MHz, $CDCl_3$, 23 °C): δ = = 7.22 (t, J = 7.8 Hz, 1 H, CH_{PhOH}), 7.06 (d, J = 7.3 Hz, 1 H, CH_{PhOH}), 6.8 (m, 4 H, H_{Ar}), 6.70 (s, 2 H, CH_{Im}), 3.91 (s, 1 H, CH_{aminal}), 3.78 (d, J = 13.3 Hz, 2 H, CH_2-Im), 3.51 (d, J = 13.3 Hz, 2 H, CH_2-Im), 3.35 (s, 6 H, CH_3), 3.05 (m, 2 H, NCH_2CH_2N), 2.79 (m, 2 H, NCH_2CH_2N) ppm. ^{13}C NMR (90.6 MHz, $CDCl_3$, 23 °C): δ = 157.8 (C_{Ar}-OH), 144.0 (C_{quatIm}), 131.2, 130.4, 119.0, and 116.6 ($C_{PhOH}H$), 127.1 and 121.7 ($C_{Im}H$), 120.6 ($C_{quatPhOH}$), 88.1 (CH_{aminal}), 49.6 and 48.0 (CH_2C_{Im}, N-CH_2-CH_2-N), 32.4 (Me) ppm. ES-MS: *m*/*z* (%) 353.4 (100) $[M + H]^+$.

***N*-(2-Hydroxybenzyl)-*N*,*N*′-bis[2-(*N*-methylimidazolyl)methyl]ethane-1,2-diamine (LH):** $NaBH_3CN$ (0.107 g, 1.70 mmol, 1 equiv.) and then CF_3COOH (0.390 g, 340 mL, 3.40 mmol, 2 equiv.) were added to a solution of **3** (0.600 g, 1.70 mmol, 1 equiv.) in absolute ethanol (30 mL). After stirring for 2 h, 1 M NaOH (10 mL) was added and the ethanol was evaporated. CH_2Cl_2 (20 mL) was then added and the pH adjusted to 9 by addition of 1 M HCl. The organic phase was decanted and the aqueous phase extracted with 3×20 mL of CH_2Cl_2. The combined organic fractions were concentrated to obtain the product as a yellow oil (0.600 g, quantitative yield). ^{1}H NMR (300 MHz,$CDCl_3$, 23 °C): δ = 7.18 (t, J = 7.5 Hz, 1 H, H_{Ar}), 6.92 (d, J = 7.5 Hz, 1 H, H_{Ar}), 6.8 (m, 6 H, H_{Ar}), 3.74 (s, 2 H, N-CH_2-C_{Ar}), 3.71, (s, 2 H, N-CH_2-C_{Ar}), 3.70 (s, 2 H, N-CH_2-C_{Ar}), 3.58 (s, 3 H, N-CH_3), 3.40 (s, 3 H, N-CH_3), 2.78 (m, 4 H, CH_2-CH_2) ppm. ^{13}C NMR (75.5 MHz, $CDCl_3$, 23 °C): δ = 157.0 (C_{Ar}-OH), 145.1 and 144.7 (C_{quatIm}), 130.1, 128.6, 126.3, 122.7, 121.0, 120.7, 118.4, and 116.1 (C_{Ar}-H), 123.1 ($C_{quatPhOH}$), 56.1, 51.6, 49.3, 45.4, and 43.4 (CH_2), 32.8 and 32.3 (N-CH_3) ppm. ES-MS: *m*/*z* (%) 355.3 $[M + H]^+$ (100). IR (KBr pellet): $\tilde{\nu}_{max}$ = 757 ($\delta_{imidazol}$), 1282 (ν_{C-O}), 1454 and 1487 cm^{-1} ($\nu_{C=N}$).

$[Mn_2(L)_2](PF_6)_2$: NEt_3 (16 mg, 21 μL, 0.155 mmol, 0.5 equiv.) was added to a solution of LH (0.110 g, 0.310 mmol, 1 equiv.) in MeOH (40 mL) and argon was bubbled into the solution to remove O_2. A deoxygenated solution of $MnBr_2$ (67 mg, 0.310 mmol, 1 equiv.) in MeOH (10 mL) was added to this mixture and the solution heated at 50 °C for 30 min. A deoxygenated solution of NH_4PF_6 (101 mg, 0.621 mmol, 2 equiv.) in methanol (1 mL) was then added and the resulting solution allowed to cool overnight. The complex started to crystallize out of solution, and 92 mg (40% yield) of nearly colorless crystals were isolated by filtration. ES-MS [dilute aqueous solution (5×10^{-5} M and 5×10^{-6} M)]: *m*/*z* (%) 408.6 $[(L)Mn]^+$ (100), 353.3 $[LH + H]^+$ (23). The peak separation within the 408.6 mul-

tiplet is +1, which indicates a +1 charge and is consistent with the monometallic species $[(L)Mn]^+$. IR (KBr pellet): $\tilde{\nu}_{max}$ = 760 ($\delta_{imidazol}$), 837 (PF_6), 1290 (ν_{C-O}), 1447 and 1484 cm^{-1} ($\nu_{C=N}$). $C_{38}H_{50}F_{12}Mn_2N_{12}O_2P_2$ (1106.7): calcd. C 41.24, H 4.55, Mn 9.93, N 15.19, P 5.60; found C 40.99, H 4.61, Mn 9.36, N 14.98, P 5.48.

Magnetic Measurements and Fitting Procedures: Magnetization data were collected for ground crystals with a Quantum Design MPMS5 magnetometer in the 2–300 K temperature region (applied field: 10 kG). The data were corrected for the diamagnetism contributions of the sample and of the cell. At 300 K, χT = 8.01 $cm^3 K mol^{-1}$. This value remained constant down to about 50 K upon lowering the temperature and then decreased abruptly to a value of 0.65 $cm^3 K mol^{-1}$ at 2 K. This behavior is indicative of an antiferromagnetic coupling between the two Mn^{II} ions. The experimental data were fitted to the expression for a dinuclear Mn^{II} (S_1 = 5/2)–Mn^{II} (S_2 = 5/2) complex using the Hamiltonian $H = -JS_1S_2$ (Marquardt algorithm from KaleidaGraph). A g-value of 1.94 was obtained from the fitting of $\chi T = f(T)$ at high temperatures. A J-value of –0.9 cm^{-1} was obtained by fitting $\chi = f(T)$ using g = 1.94. As shown in Figure 8, a good agreement was obtained for $\mathbf{1}(PF_6)_2$ in the whole temperature range for both χT and χ.

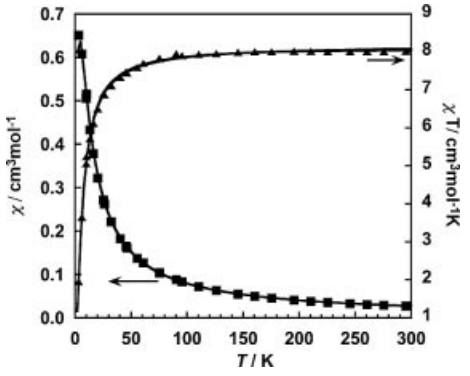

Figure 8. Thermal variation of χT (triangles) and χ (squares) vs. temperature for $\mathbf{1}(PF_6)_2$. For clarity, only 30% of the recorded data are shown. The solid lines correspond to the data calculated with the parameters g = 1.94 and J = –0.9 cm^{-1} with $H = -JS_1S_2$.

X-ray Crystallography: X-ray diffraction data for $\mathbf{1}(PF_6)_2$ were collected with a Kappa X8 APPEX II Bruker diffractometer with graphite-monochromated Mo-K_α radiation (λ = 0.71073 Å) and corrected for Lorentz, polarization, and absorption effects. The structures were solved by direct methods using SHELXS-97[83] and refined against F^2 by full-matrix least-squares techniques using SHELXL-97[84] with anisotropic displacement parameters for all non-hydrogen atoms. Hydrogen atoms were located on a difference Fourier map and introduced into the calculations as a riding model with isotropic thermal parameters. All calculations were performed with the crystallographic software package WINGX.[85] The crystal data collection and refinement parameters are given in Table 3.

CCDC-622751 contains the supplementary crystallographic data for this paper. These data can be obtained free of charge from the Cambridge Crystallographic Data Centre via www.ccdc.cam.ac.uk/data_request/cif.

SOD Activity Measurements: The assay and controls to ensure reliability were performed as described previously.[24,27] The standard conditions used were: T = 25 °C (potassium phosphate buffer, 50 mM, pH 7.8 or PIPES, 50 mM, pH 7.5),[38] [xanthine] = 200 μM and a quantity of xanthine oxidase ensuring a ΔA of at least 0.025 min^{-1}. The reduction of ferricytochrome c at 550 nm was monitored first in the absence of any putative SOD mimic and then after addition of the mimic. The slope of the line $A_{550nm} = f(t)$ before addition of the SOD mimic is s_1 and s_2 is the slope after addition of the SOD mimic. $(s_1 - s_2)/s_2$ was plotted against the complex concentration to provide a line and the IC_{50} was then obtained for $(s_1 - s_2)/s_2 = 1$. Experiments were performed in duplicate for each buffer.

Table 3. Crystallographic data for $\mathbf{1}(PF_6)_2$.

Formula	$C_{38}H_{50}Mn_2N_{12}O_2 \cdot 2(PF_6)$
Fw	1106.72
Crystal system	triclinic
Space group	$P\bar{1}$
a [Å]	9.2677(12)
b [Å]	11.0617(14)
c [Å]	13.2606(16)
α [°]	107.965(2)
β [°]	107.114(3)
γ [°]	92.810(3)
V [Å^3]	1221.2(3)
Z	1
F(000)	566
λ [Å]	0.71073
T [K]	273(2)
$\rho_{calcd.}$ [$Mg m^{-3}$]	1.505
μ(Mo-K_α) [mm^{-1}]	0.675
Crystal size [mm^3]	$0.20 \times 0.14 \times 0.06$
θ range [°]	3.00–26.19
Number of data collected	6141
Number of unique data	3291
R(int)	0.0252
Absorption correction	SADABS
Number of variable parameters	307
Number of observed reflections[a]	2639
R[b] obsd., all	0.0565, 0.0702
R_w[c] obsd., all	0.1671, 0.1795
S	1.075
Largest diff. peak and hole [e Å^{-3}]	0.805, –0.450

[a] Data with $F_o > 4\sigma(F_o)$. [b] $R = \Sigma||F_o|-|F_c||/\Sigma|F_o|$. [c] $R_w = [\Sigma w(|F_o^2|-|F_c^2|)^2/\Sigma w|F_o^2|^2]^{1/2}$.

Supporting Information (see footnote on the first page of this article): Figure S1, Evolution of the cyclic voltammogram of $[\mathbf{1}(PF_6)_2]$ upon addition of base (2,6-lutidine).

Acknowledgments

We thank Eric Rivière for recording the magnetic measurements and Geneviève Blondin for useful discussions on the EPR spectroscopy. This work was supported by the French government (grant no. ACI-2004 JC2044 to C. P.).

[1] B. Halliwell, J. M. C. Gutteridge, *Free Radicals in Biology and Medicine*, Oxford University Press, New York, **1999**.
[2] D. P. Riley, *Chem. Rev.* **1999**, *99*, 2573–2587.
[3] D. Salvemini, C. Muscoli, D. P. Riley, S. Cuzzocrea, *Pulm. Pharmacol. Ther.* **2002**, *15*, 439–447.
[4] J. M. McCord, M. A. Edeas, *Biomed. Pharmacother.* **2005**, *59*, 139–142.
[5] P. R. Gardner, I. Raineri, L. B. Epstein, C. W. White, *J. Biol. Chem.* **1995**, *270*, 13399–13405.
[6] P. R. Gardner, I. Fridovich, *J. Biol. Chem.* **1992**, *267*, 8757–8763.
[7] F. S. Archibald, I. Fridovich, *J. Bacteriol.* **1981**, *145*, 442–451.

[8] R. J. Sanchez, C. Srinivasan, W. H. Munroe, M. A. Wallace, J. Martins, T. Y. Kao, K. Le, E. B. Gralla, J. S. Valentine, *J. Biol. Inorg. Chem.* **2005**, *10*, 913–923.
[9] M. Al-Maghrebi, I. Fridovich, L. Benov, *Arch. Biochem. Biophys.* **2002**, *402*, 104–109.
[10] M. Baudry, S. Etienne, A. Bruce, M. Palucki, E. Jacobsen, B. Malfroy, *Biochem. Biophys. Res. Commun.* **1993**, *192*, 964–968.
[11] A. Puglisi, G. Tabb, G. Vecchio, *J. Inorg. Biochem.* **2004**, *98*, 969–976.
[12] T. Magwere, M. West, K. Riyahi, M. P. Murphy, R. A. J. Smith, L. Partridge, *Mech. Ageing Dev.* **2006**, *127*, 356–370.
[13] J. D. Rush, Z. Maskos, W. H. Koppenol, *Arch. Biochem. Biophys.* **1991**, *289*, 97–102.
[14] D. P. Riley, R. H. Weiss, *J. Am. Chem. Soc.* **1994**, *116*, 387–388.
[15] D. P. Riley, S. L. Henke, P. J. Lennon, R. H. Weiss, W. L. Neumann, W. J. J. Rivers, K. W. Aston, K. R. Sample, H. Rahman, C.-S. Ling, J.-J. Shieh, D. H. Busch, W. Szulbinski, *Inorg. Chem.* **1996**, *35*, 5213–5231.
[16] D. P. Riley, S. L. Henke, P. J. Lennon, K. Aston, *Inorg. Chem.* **1999**, *38*, 1908–1917.
[17] D. Salvemini, Z.-Q. Wang, J. L. Zweier, A. Samouilov, H. Macarthur, T. P. Misko, M. G. Currie, S. Cuzzocrea, J. A. Sikorski, D. P. Riley, *Science* **1999**, *286*, 304–305.
[18] R. D'Agata, G. Grasso, G. Iacono, G. Spoto, G. Vecchio, *Org. Biomol. Chem.* **2006**, *4*, 610–612.
[19] A. Dees, A. Zahl, R. Puchta, N. J. R. Van Eikema Hommes, F. W. Heinemann, I. Ivanovic-Burmazovic, *Inorg. Chem.* **2007**, *46*, 2459–2470.
[20] N. Kitajima, M. Osawa, N. Tamura, Y. Moro-Oka, T. Hirano, M. Hirobe, T. Nagano, *Inorg. Chem.* **1993**, *32*, 1879–1880.
[21] A. Deroche, I. Morgenstern-Badarau, M. Cesario, J. Guilhem, B. Keita, L. Nadjo, C. Houée-Levin, *J. Am. Chem. Soc.* **1996**, *118*, 4567–4573.
[22] D. F. Xiang, X. S. Tan, Q. W. Hang, W. X. Tang, B.-M. Wu, T. C. W. Mak, *Inorg. Chim. Acta* **1998**, *277*, 21–25.
[23] K. Yamato, I. Miyahara, A. Ichimura, K. Hirotsu, Y. Kojima, H. Sakurai, D. Shiomi, K. Sato, T. Takui, *Chem. Lett.* **1999**, 295–296.
[24] C. Policar, S. Durot, F. Lambert, M. Cesario, F. Ramiandrasoa, I. Morgenstern-Badarau, *Eur. J. Inorg. Chem.* **2001**, 1807–1818.
[25] E. A. Lewis, H. H. Khodr, R. C. Hider, J. R. Lindsay-Smith, P. H. Walton, *Dalton Trans.* **2004**, 187–188.
[26] S. Durot, F. Lambert, J.-P. Renault, C. Policar, *Eur. J. Inorg. Chem.* **2005**, 2789–2793.
[27] S. Durot, C. Policar, F. Cisnetti, F. Lambert, J.-P. Renault, G. Pelosi, G. Blain, H. Korri-Youssoufi, J.-P. Mahy, *Eur. J. Inorg. Chem.* **2005**, 3513–3523.
[28] F. Cisnetti, G. Pelosi, C. Policar, *Inorg. Chim. Acta* **2007**, *360*, 557–562.
[29] Z.-R. Liao, X.-F. Zheng, B.-S. Luo, L.-R. Shen, D.-F. Li, H.-L. Liu, W. Zhao, *Polyhedron* **2001**, *20*, 2813–2821.
[30] J. Alexandre, C. Nicco, C. Chéreau, A. Laurent, B. Weill, F. Goldwasser, F. Batteux, *J. Natl. Cancer Inst.* **2006**, *98*, 236–244.
[31] H. Brurok, J. H. Ardenkjaer-Larsen, G. Hansson, S. Skarra, K. Berg, J. O. G. Karlsson, I. Laursen, P. Jynge, *Biochem. Biophys. Res. Commun.* **2006**, *254*, 768–772.
[32] S. Groni, G. Blain, R. Guillot, C. Policar, E. Anxolabéhère-Mallart, *Inorg. Chem.* **2007**, *46*, 1951–1953.
[33] W. F. Beyer, I. Fridovich, *Arch. Biochem. Biophys.* **1989**, *271*, 149–156.
[34] K. M. Faulkner, R. D. Stevens, I. Fridovich, *Arch. Biochem. Biophys.* **1994**, *310*, 341–346.
[35] J. Lati, D. Meyerstein, *J. Chem. Soc. Dalton Trans.* **1978**, 1105–1118.
[36] J. Stein, J. P. Fackler, G. J. McClune, J. A. Fee, L. T. Chan, *Inorg. Chem.* **1979**, *18*, 3511–3518.
[37] W. H. Koppenol, F. Levine, T. L. Hatmaker, J. Epp, J. D. Rush, *Arch. Biochem. Biophys.* **1986**, *251*, 594–599.
[38] F. S. Archibald, I. Fridovich, *Arch. Biochem. Biophys.* **1982**, *214*, 452–463.
[39] M. A. Bailey, M. J. Ingram, D. P. Naughton, *Biochem. Biophys. Res. Commun.* **2004**, *317*, 1155–1158.
[40] A. E. O. Fisher, D. P. Naughton, *Biomed. Pharmacother.* **2005**, *59*, 158–162.
[41] T. Piacham, C. Isarankura-Na-Ayudhya, C. Nantasenamat, S. Yainoy, L. Ye, L. Bülow, N. Prachayasittihul, *Biochem. Biophys. Res. Commun.* **2006**, *341*, 925–930.
[42] J. S. Valentine, A. E. Quinn, *Inorg. Chem.* **1976**, *15*, 1997–1999.
[43] K. M. Faulkner, S. I. Liochev, I. Fridovich, *J. Biol. Chem.* **1994**, *269*, 23471–23476.
[44] I. Batinic-Haberle, S. I. Liochev, I. Spasojevic, I. Fridovich, *Arch. Biochem. Biophys.* **1997**, *343*, 225–233.
[45] I. Batinic-Haberle, L. Benov, I. Spasojevic, I. Fridovich, *J. Biol. Chem.* **1998**, *273*, 24521–24528.
[46] P. J. F. Gauuan, M. P. Trova, L. Gregor-Boros, S. B. Bocckino, J. D. Crapo, B. J. Day, *Bioorg. Med. Chem.* **2002**, *10*, 3013–3021.
[47] I. Batinic-Haberle, I. Spasojevic, R. D. Stevens, B. Bondurant, A. Okado-Matsumoto, I. Fridovich, Z. Vujaskovic, M. W. Dewhirsta, *Dalton Trans.* **2006**, 617–624.
[48] I. Spasojevic, I. Batinic-Haberle, R. D. Stevens, P. Hambright, A. N. Thorpe, J. Grodkowski, P. Neta, I. Fridovich, *Inorg. Chem.* **2001**, *40*, 726–739.
[49] G. O. E. Borgstahl, H. E. Parge, M. J. Hickey, W. F. Beyer, R. A. Hallewell, J. A. Tainer, *Cell* **1992**, *71*, 107–118.
[50] C. Hureau, E. Anxolabéhère-Mallart, M. Nierlich, F. Gonnet, E. Rivière, G. Blondin, *Eur. J. Inorg. Chem.* **2002**, 2710–2719.
[51] C. Hureau, L. Sabater, E. Anxolabéhère-Mallart, M. Nierlich, M.-F. Charlot, F. Gonnet, E. Rivière, G. Blondin, *Chem. Eur. J.* **2004**, *10*, 1998–2010.
[52] C. Baffert, M.-N. Collomb, A. Deronzier, S. Kjærgaard-Knudsen, J.-M. Latour, C. H. Lund, C. J. McKenzie, M. Mortensen, L. P. Nielsen, N. Thorup, *Dalton Trans.* **2003**, 1765–1772.
[53] P. E. Iberson, H. Lund, *Acta Chem. Scand.* **1966**, *20*, 2649.
[54] F. J. Laronde, M. A. Brooks, *Inorg. Chim. Acta* **1999**, *296*, 208–221.
[55] J. Brinskma, M. T. Rispens, R. Hage, B. L. Feringa, *Inorg. Chim. Acta* **2002**, 75–82.
[56] C. F. Macrae, P. R. Edington, P. R. McCabe, E. Pidcock, G. P. Shields, R. Taylor, M. Towler, J. Van De Streek, *J. Appl. Crystallogr.* **2006**, *39*, 453–457.
[57] M. G. B. Drew, C. J. Harding, V. McKee, G. G. Morgan, J. Nelson, *J. Chem. Soc. Chem. Commun.* **1995**, 1035–1038.
[58] D. P. Kessissoglou, W. M. Butler, V. L. Pecoraro, *Inorg. Chem.* **1987**, *26*, 195–203.
[59] H. Adams, N. A. Bailey, N. A. Debaecker, D. E. Fenton, W. Kanda, J.-M. Latour, H. Okawa, H. Sakiyama, *Angew. Chem. Int. Ed. Engl.* **1995**, *34*, 2535–2537.
[60] B. E. Schultz, B.-H. Ye, X.-Y. Li, S. I. Chan, *Inorg. Chem.* **1997**, *36*, 2617–2622.
[61] T. Howard, J. Tesler, V. J. Derose, *Inorg. Chem.* **2000**, *39*, 3379–3385.
[62] S. Blanchard, G. Blain, E. Rivière, M. Nierlich, G. Blondin, *Chem. Eur. J.* **2003**, *9*, 4260–4268.
[63] S. Blanchard, G. Blondin, E. Rivière, M. Nierlich, J. J. Girerd, *Inorg. Chem.* **2003**, *42*, 4568–4578.
[64] $E_{1/2} = 1/2[E_p^a + E_p^c]$.
[65] L. Sabater, C. Hureau, G. Blain, R. Guillot, P. Thuery, E. Rivière, A. Aukaulo, *Eur. J. Inorg. Chem.* **2006**, 4324–4337.
[66] A. Neves, S. M. D. Erthal, I. Vencato, A. S. Ceccato, Y. P. Mascarenhas, O. R. Nascimento, M. Horner, A. A. Batista, *Inorg. Chem.* **1992**, *31*, 4749–4755.
[67] H. Diril, H.-R. Chang, M. J. Nilges, X. Zhang, J. A. Potenza, H. J. Schugar, S. S. Isied, D. N. Hendrickson, *J. Am. Chem. Soc.* **1989**, *111*, 5102–5114.
[68] J. A. Bonadies, M. J. Maroney, V. L. Pecoraro, *Inorg. Chem.* **1989**, *28*, 2044–2797.

[69] 2,6-Lutidine was chosen based on previous reports by Hureau et al.[50,51].
[70] N. E. Good, G. D. Winget, W. Winter, T. N. Connolly, S. Izawa, R. M. M. Singh, *Biochemistry* **1966**, *5*, 467–477.
[71] C. Policar, I. Artaud, D. Mansuy, *Inorg. Chem.* **1996**, *35*, 210–216.
[72] R. D. Dowsing, J. F. Gibson, D. M. L. Goodgame, M. Goodgame, P. J. Hayward, *Nature* **1968**, *219*, 1037–1038.
[73] R. D. Dowsing, J. F. Gibson, M. Goodgame, P. J. Hayward, *J. Chem. Soc. C* **1969**, 187–193.
[74] E. J. Laskowski, D. N. Hendrickson, *Inorg. Chem.* **1978**, *17*, 457–470.
[75] J. M. McCord, I. Fridovich, *J. Biol. Chem.* **1969**, *244*, 6049–6055.
[76] R. F. Pasternack, B. Halliwell, *J. Am. Chem. Soc.* **1979**, *101*, 1026–1031.
[77] J. Butler, W. H. Koppenol, E. Margoliash, *J. Biol. Chem.* **1982**, *257*, 10747–10750.
[78] It should be noted that the kinetic constant for the reaction between ferricytochrome c in PIPES at pH 7.5 has not been measured, but the fact that the IC_{50} values are very close in PIPES at pH 7.5 and phosphate buffer at pH 7.8 suggests that the k_{cytC} (pH 7.5, PIPES 50 mM, 21 °C) should be very close to that reported in phosphate buffer.
[79] Y. Sawada, I. Yamazaki, *Biochem. Biophys. Acta* **1973**, *327*, 257–265.
[80] For a more exhaustive comparison with the Mn complexes from the literature, see ref.[27]
[81] W. C. J. Barrette, D. T. Sawyer, J. A. Fee, K. Asada, *Biochemistry* **1983**, *22*, 624–627.
[82] I. Batinic-Haberle, I. Spasojevic, R. D. Stevens, P. Hambright, P. Neta, A. Okado-Matsumoto, I. Fridovich, *Dalton Trans.* **2004**, 1696–1702.
[83] G. M. Sheldrick, *SHELXS-97, Program for Crystal Structure Solution*, University of Göttingen, Germany, **1990**.
[84] G. M. Sheldrick, *SHELXL 97, Program for the refinement of crystal structures from diffraction data*, University of Göttingen, Germany, **1997**.
[85] L. J. Farrugia, *J. Appl. Crystallogr.* **1999**, *32*, 837–838.

Received: December 22, 2006
Published Online: August 9, 2007

